Spatial correlations in dynamical mean-field theory

J. Lleweilun Smith and Qimiao Si
Department of Physics, Rice University, Houston, Texas 77251-1892
(Received 4 March 1999)

We further develop an extended dynamical mean-field approach introduced earlier. It goes beyond the standard $D=\infty$ dynamical mean field theory by incorporating quantum fluctuations associated with intersite (Ruderman-Kittel-Kasuya-Yosida like) interactions. This is achieved by scaling the intersite interactions to the same power in $1/D$ as that for the kinetic terms. In this approach, a correlated lattice problem is reduced to a single-impurity Anderson model with additional self-consistent bosonic baths. Here, we formulate the approach in terms of standard perturbation expansions. We show that the two-particle vertex functions are momentum-dependent, while the single-particle self-energy remains local. In spite of this, the approach is conserving. Finally, we also determine the form of a momentum-dependent dynamical susceptibility; the resulting expression relates it to the corresponding Weiss field, local correlation function and (momentum-dependent) intersite coupling.

I. INTRODUCTION

In strongly correlated electron systems, both local and nonlocal interactions are important in determining the nature of the ground state and low-lying excitations. One example illustrating this point comes from Kondo systems, such as heavy fermions. Here, the competition between the local Kondo interactions and nonlocal Ruderman-Kittel-Kasuya-Yosida (RKKY) interactions was recognized to play an essential role from very early on.[1,2] The Kondo effect tends to quench local moments altogether, while the RKKY interactions promote magnetic ordering. What happens when the two processes are about ''equally'' important is an intriguing question that remains poorly understood. This question has once again become centrally important, due to the emergence of a host of heavy fermion metals lying in the vicinity of a quantum phase transition.[3]

The interplay between local and nonlocal interactions is also essential in Mott-Hubbard systems.[4] When on-site interactions are strong, their effects can be thought of as determining the atomic configurations that lie at low energies. The precise form of the ground state and low-lying excitations, on the other hand, have to be determined by the residual intersite couplings between these low-energy configurations.

In general, a separation of electron-electron interactions into local and nonlocal ones is not necessarily well defined. Local interactions, when combined with kinetic terms, can lead to effective nonlocal interactions. After all, both RKKY and super-exchange interactions arise in this fashion.

In theoretical approaches, however, such a separation can often be sharply defined. In this paper, we are concerned with the dynamical mean field theory[5] (DMFT), which is formally exact in the limit of infinite dimensions ($D=\infty$).[6] The DMFT reduces a correlated lattice problem to a self-consistent Anderson impurity model, namely a quantum impurity coupled to a self-consistent fermionic bath. The interactions between the impurity degrees of freedom reflect the on-site interactions of the lattice problem; in this way local quantum fluctuations are retained. The self-consistent fermionic bath of the impurity problem reflects the influence, at the one-particle level, of the rest of the lattice on the selected (i.e., impurity) site. All the intersite correlations of the lattice problem, on the other hand, are neglected. In this sense, nonlocal quantum fluctuations are completely lost.

In earlier works, we[7,8] and independently Kajueter and Kotliar[9] have extended the DMFT such that intersite quantum fluctuations are treated on an equal footing with local ones. This extended DMFT reduces a correlated lattice problem into a novel effective impurity problem, which corresponds to an Anderson impurity model with additional self-consistent bosonic baths. These bosonic baths reflect the influence, at the two-particle level, of the rest of the lattice on the impurity site. In the magnetic case, for instance, they represent the fluctuating magnetic fields induced by the intersite spin-exchange interactions. Through self-consistency, they keep track of the intersite quantum fluctuations. In these earlier works, the mean-field equations were derived using the so-called ''cavity'' method.

The purpose of this paper is to give an alternative formulation of this extended DMFT using diagrammatic perturbation methods. Using the new formulation, we are able to establish the conserving nature of this approach and also derive the expressions for momentum-dependent correlation functions. These expressions specify how to calculate the correlation functions from the corresponding Weiss fields, local correlation functions and (momentum-dependent) intersite interactions.

To be specific, we focus on a one band model,

$$H=\sum_i Un_{i\uparrow}n_{i\downarrow}+\sum_{\langle ij\rangle,\sigma} t_{ij}c_{i\sigma}^{\dagger}c_{j\sigma} -\frac{1}{2}\sum_{\langle ij\rangle} v_{ij}(n_i-\langle n\rangle)(n_j-\langle n\rangle)-\frac{1}{2}\sum_{\langle ij\rangle} J_{ij}\vec{S}_i\cdot\vec{S}_j . \quad (1)$$

The first two terms alone would correspond to the standard Hubbard model for a spin 1/2 band. The third and forth terms are the intersite density-density (v_{ij}) and spin-exchange

(J_{ij}) interactions. Here n_i and $\vec{S}_i$ are the density and spin operators for the c electrons. $\langle ij \rangle$ labels a pair of nearest-neighbor sites. For simplicity, we limit both the hopping and intersite-interaction terms to nearest-neighbor only. Generalizing to the case with longer-range hopping and interaction terms is straightforward.

In the standard large D approach, the single-electron hopping term is taken to be of order $1/\sqrt{D}$:

$$t_{\langle ij \rangle} = t/\sqrt{D}. \tag{2}$$

The large D limit leads to an effective single-site problem, which describes an impurity coupled to a self-consistent Weiss field. There is one Weiss field for each frequency, due to the quantum-mechanical nature of the hopping term. The coupling of the impurity to this frequency-dependent Weiss field can be equivalently described in terms of a coupling between the impurity and an effective noninteracting fermionic bath. The bath is fermionic, since the Weiss field describes the influence of the rest of sites to the selected impurity site at the one-particle level. On the other hand, the intersite interaction terms (both $v_{\langle ij \rangle}$ and $J_{\langle ij \rangle}$) are taken to be of order $1/D$. With such scaling, only the static Hartree contributions survive the large D limit.[10] All the quantum fluctuations associated with these interactions are then neglected.

In the extended DMFT, these intersite interaction terms are also scaled to the order $1/\sqrt{D}$. The large D limit then leads to a different effective impurity problem: the impurity is now also coupled to the frequency-dependent Weiss fields induced by these intersite interactions. The two-particle nature of the intersite interactions dictate the bosonic nature of the corresponding effective baths in the impurity problem. As a result, the effective single-site problem can be thought of as an impurity coupled not only to a self-consistent fermionic bath but also to self-consistent bosonic baths.

The rest of the paper is organized as follows. In Sec. II, we introduce the extended large D limit and derive the mean-field equations using perturbation methods. We then derive the expressions for the momentum-dependent correlation functions in Sec. III. The proof that the approach is conserving is given in Sec. IV. In Sec. V, we (a) generalize the approach to multiband systems as well as to the case of an ordered state; (b) specify an approximate procedure to deal with incommensurate spatial fluctuations; and finally (c) compare our approach with others within the general DMFT framework.

II. THE EXTENDED DYNAMICAL MEAN-FIELD APPROACH

In this section, we introduce the extended large D limit and derive the mean-field equations.

The intersite hopping term, $t_{\langle ij \rangle}$, remains of order $1/\sqrt{D}$ as given in Eq. (2). The nearest-neighbor interactions are now scaled to the same order,

$$v_{\langle ij \rangle} = v/\sqrt{D}$$
$$J_{\langle ij \rangle} = J/\sqrt{D}. \tag{3}$$

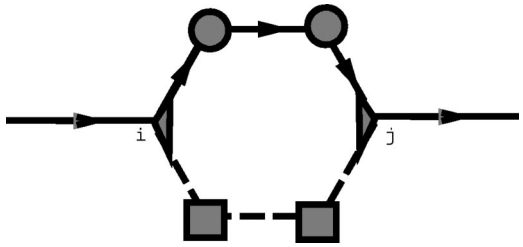

FIG. 1. A typical intersite self-energy diagram. A full line represents a single-particle Green's function, and a dashed line corresponds to an intersite interaction. This diagram is subleading.

In order for the large D limit to be well defined, we need to subtract the Hartree contribution as has already been done in Eq. (1). (The normal-ordering notation $:\eta:$ will be used to denote $\eta - \langle \eta \rangle$.)

We now establish that the self-energy is still local. Consider first the self-energy $\Sigma_{\langle ij \rangle}$. The Hartree contributions from both $v_{\langle ij \rangle}$ and $J_{\langle ij \rangle}$ vanish. The Fock and high-order contributions to the self-energy can be written in a skeleton expansion. As illustrated in Fig. 1, any skeleton expansion diagram for the self-energy contains at least an intersite interaction path and a fermion propagator from site i to site j. Both are at least of order $1/\sqrt{D}$. Therefore, $\Sigma_{\langle ij \rangle} \sim O(1/D)$. More generally, $\Sigma_{ij} \sim O(1/D)^{||i-j||}$, where $||i-j||$ is the least number of steps from site i to site j. This implies that in the large D limit the self-energy is momentum-independent: $\Sigma(\mathbf{q}, \omega) = \Sigma_{ii}(\omega)$.

Consider now the on-site self energy $\Sigma_{ii}(\omega)$. The only real-space self-energy diagrams that survive the large D limit have the form illustrated in Fig. 2(a), as explained in detail in Appendix B. Here a solid line represents the fermion propagator, G_{ii}. A dashed line denotes the intersite interaction (either v_{ij} or J_{ij}). The loop formed by two dashed lines enclosing a solid square is denoted as either $\chi^{-1}_{ch,0}(\omega)$ or $\chi^{-1}_{s,0}(\omega)$, which, as explained in Appendix B, has the following form,

$$\chi^{-1}_{ch,0} = \sum_{ij} v_{i0} v_{0j} (\chi_{ch,ij} - \chi_{ch,i0}\chi_{ch,0j}/\chi_{ch,loc})$$
$$\chi^{-1}_{s,0} = \sum_{ij} J_{i0} J_{0j} (\chi_{s,ij} - \chi_{s,i0}\chi_{s,0j}/\chi_{s,loc}), \tag{4}$$

where χ_{ch} and χ_s are the charge and spin susceptibilities, respectively. More specifically, they are the Fourier transforms of $\langle T_\tau :\eta_i:(\tau) :\eta_g:(0) \rangle$ and $\langle T_\tau \vec{S}_i(\tau) \cdot \vec{S}_j(0) \rangle$, respectively.

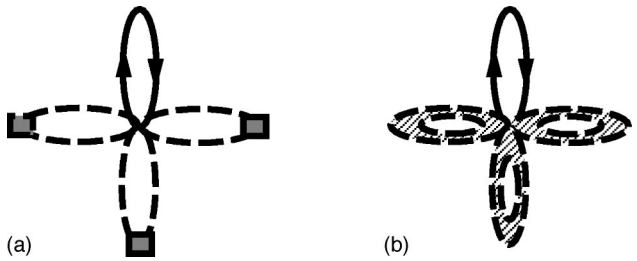

FIG. 2. (a) An on-site self-energy diagram of the lattice problem. (b) The corresponding local self-energy diagram of the effective impurity problem. A shaded line corresponds to a Weiss field.

The above implies that Σ_{ii} can be equivalently calculated in terms of a local problem with an action of the following form,

$$S^{MF}=\int_0^\beta d\tau U n_\uparrow(\tau)n_\downarrow(\tau)-\int_0^\beta d\tau\int_0^\beta d\tau' \times\Bigg[\sum_\sigma c_\sigma^\dagger(\tau)G_0^{-1}(\tau-\tau')c_\sigma(\tau')+:n(\tau):\chi_{ch,0}^{-1} \times(\tau-\tau'):n(\tau'):+\vec{S}(\tau)\cdot\chi_{s,0}^{-1}(\tau-\tau')\vec{S}(\tau')\Bigg], \quad (5)$$

where $:n:\equiv n-\langle n\rangle$. The skeleton expansion for the self-energy of this local problem, Σ_{loc}, has the form given in Fig. 2(b) where a solid line represents G_{loc} and a shaded line represents either $\chi_{ch,0}^{-1}$ or $\chi_{s,0}^{-1}$. Since there exists a one-to-one correspondence between the diagrams in Figs. 2(a) and 2(b), we have

$$\Sigma_{loc}=\Sigma_{ii} \quad (6)$$

if G_0 is chosen such that

$$G_{loc}=G_{ii}. \quad (7)$$

In standard fashion,[5] it can be seen from the Dyson equations for both the local problem and the lattice problem that, Eqs. (6) and (7) are satisfied if the Weiss field is chosen as

$$G_0^{-1}(i\omega_n)=i\omega_n+\mu-\sum_{ij} t_{i0}t_{0j}[G_{ij}(i\omega_n) -G_{i0}(i\omega_n)G_{0j}(i\omega_n)/G_{loc}(i\omega_n)]. \quad (8)$$

Consider now the higher-order correlation functions. In a skeleton expansion for any on-site correlation function of the lattice problem, every diagram also has the form of Fig. 2(a) [with even(odd) number of fermion loops for any even(odd)-number-particle correlation functions]. Likewise, the skeleton expansion diagrams for the corresponding local correlation function of the impurity problem have the structure of Fig. 2(b). As a result Eqs. (4) and (7), or equivalently, Eqs. (4) and (8), also guarantee that all the on-site higher-order correlation functions of the lattice problem can be calculated from the effective impurity problem. In particular, $\chi_{ch,loc}=\chi_{ch,ii}$ and $\chi_{s,loc}=\chi_{s,ii}$.

Equations (5), (8), and (4) form the self-consistency equations. The effective impurity problem, defined by the action given in Eq. (5), can be equivalently written in terms of an impurity Hamiltonian of the following form,

$$H_{imp}=H_{kin}+E_d\sum_\sigma c_\sigma^\dagger c_\sigma+Un_{c\uparrow}n_{c\downarrow}+t\sum_{k\sigma}(c_\sigma^\dagger\eta_{k\sigma}+\text{H.c.}) +F\sum_q :n_c:(\rho_q+\rho_{-q}^\dagger)+g\sum_q \vec{S}_c\cdot(\vec{\phi}_q+\vec{\phi}_{-q}^\dagger)$$
$$H_{kin}=\sum_{k\sigma} E_k\eta_{k\sigma}^\dagger\eta_{k\sigma}+\sum_q W_q\rho_q^\dagger\rho_q+\sum_q w_q\vec{\phi}_q^\dagger\cdot\vec{\phi}_q, \quad (9)$$

where $E_d=-\mu$ and the parameters E_k, W_q, w_q, V, F, and g are given by

$$i\omega_n+\mu-t^2\sum_k 1/(i\omega_n-E_k)=G_0^{-1}(i\omega_n)$$
$$F^2\sum_q W_q/[(i\nu_n)^2-W_q^2]=\chi_{ch,0}^{-1}(i\nu_n) \quad (10)$$
$$g^2\sum_q w_q/[(i\nu_n)^2-w_q^2]=\chi_{s,0}^{-1}(i\nu_n),$$

where $i\omega_n$ and $i\nu_n$ are Matsubara frequencies for fermions and bosons, respectively.

Equation (9) describes a single-impurity Anderson model coupled to two additional bosonic bands. The impurity corresponds to the c orbital. $\eta_{k\sigma}$ is the usual fermionic bath of the Anderson model, with a dispersion of E_k. ρ_q is a scalar-bosonic bath. $\vec{\phi}_q$ corresponds to a vector-bosonic bath. Note that the different components of the vector boson commute with each other: $[\phi_q^\alpha,\phi_{q'}^{\beta,\dagger}]=\delta_{\alpha\beta}\delta_{qq'}$ where $\alpha,\beta=x,y,z$. The dispersions of the bosonic baths are W_q and w_q.

As in the usual large D limit, having solved the local problem we can then calculate the lattice Green's function

$$G(\mathbf{k},\omega)=\frac{1}{\omega+\mu-\epsilon_k-\Sigma(\omega)}. \quad (11)$$

In the following, we establish that a parallel procedure can be carried out for the lattice correlation functions.

III. MOMENTUM-DEPENDENT CORRELATION FUNCTIONS

We now specify the procedure to calculate the momentum-dependent correlation functions. For simplicity, we focus on the spin-spin correlation function only. The density-density correlation function has a similar form.

A. Two-particle vertex functions

We first establish the form of two-particle vertex functions. Consider the spin susceptibility, $\chi_s(\mathbf{q},\omega)$, which can be written as

$$\chi_s(\mathbf{q},\omega)=\int d\epsilon_1 d\epsilon_2\chi_s(\epsilon_1,\epsilon_2;\mathbf{q},\omega), \quad (12)$$

where ϵ_1, ϵ_2 are illustrated in Fig. 3, which also specifies the Bethe-Salpeter equation,

$$\chi_{s,ij}(\epsilon_1,\epsilon_2;\omega)=\chi_{ij}^{ph}(\epsilon_1;\omega)\delta_{\epsilon_1,\epsilon_2} +\int d\epsilon'\sum_{l_1,m_1,l_2,m_2}\chi_{il_1im_1}^{ph}(\epsilon_1;\omega) \times I_{l_1l_2m_1m_2}(\epsilon_1\epsilon';\omega)\chi_{s,l_2jm_2j}(\epsilon',\epsilon_2;\omega). \quad (13)$$

Here χ^{ph} represents the particle-hole bubble, with full fermion propagators. $I_{l_1m_1l_2m_2}$ is the irreducible vertex function in the triplet particle-hole channel. It follows from the counting rules of Appendix A that only a limited number of contributions on the right-hand side are of leading order. For the first term on the right-hand side, only the $i=j$ contribution is

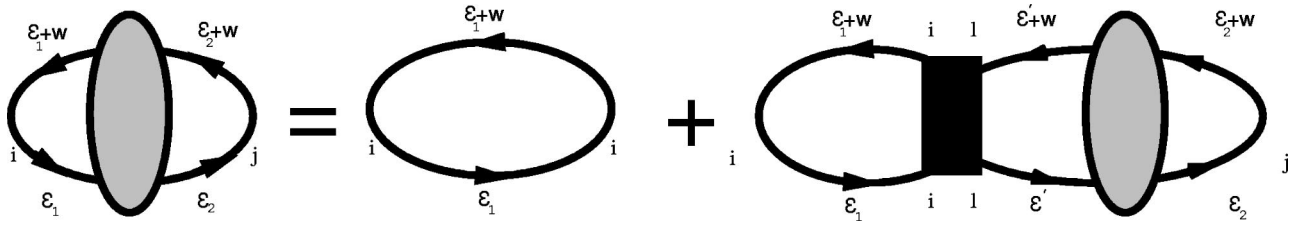

FIG. 3. The Bethe-Salpeter equation. Here a bubble with a shaded insertion represents the susceptibility. The solid square describes an irreducible vertex function.

leading. For the second term, only terms with $l_1=m_1=i$ and $l_2=m_2$ contribute. Eq. (13) then leads to

$$\chi_s(\mathbf{q},\omega)^{-1}_{\epsilon_1,\epsilon_2}=\chi^{ph}(\epsilon_1;\omega)^{-1}\delta_{\epsilon_1,\epsilon_2}-I(\epsilon_1,\epsilon_2;\mathbf{q},\omega), \tag{14}$$

where $I(\epsilon_1,\epsilon_2;\mathbf{q},\omega)\equiv\Sigma_j e^{i\mathbf{q}\cdot\mathbf{R}_{ij}}I_{ijij}(\epsilon_1,\epsilon_2;\omega)$. Note that Eq. (14) is a matrix equation, with ϵ_1,ϵ_2 specifying matrix elements.

We now need to calculate the irreducible vertex function $I(\epsilon_1,\epsilon_2;\mathbf{q},\omega)$ in terms of the effective impurity problem. To do that, we first carry out a cumulant expansion for the spin susceptibility of the lattice model. A cumulant is introduced in a perturbative expansion in terms of t_{ij}, v_{ij} and J_{ij}. It represents the corresponding local single-particle or two-particle Green's function calculated entirely in terms of the on-site (''atomic'') part of the lattice Hamiltonian. For our purpose, it is more convenient to introduce an effective spin cumulant in analogy to the one-particle effective cumulant introduced by Metzner.[11] The effective spin cumulant is defined as all the diagrams for the on-site spin susceptibility which are irreducible in terms of cutting any J_{lm} line (where l and m are arbitrary). Loosely speaking, it is the bare spin cumulant plus all the local decorations. Denoting the effective spin cumulant as $C_s(\epsilon_1,\epsilon_2;\omega)$, the leading order spin susceptibility has the structure illustrated in Fig. 4 and can be written as

$$\begin{aligned}\chi_{s,ij}(\epsilon_1,\epsilon_2;\omega)=&C_s(\epsilon_1,\epsilon_2;\omega)\delta_{ij}\\&+\sum_l\int d\epsilon'\int d\epsilon'' C_s(\epsilon_1,\epsilon';\omega)\\&\times J_{il}\chi_{s,lj}(\epsilon'',\epsilon_2;\omega),\end{aligned} \tag{15}$$

which is equivalent to

$$\chi_s(\mathbf{q},\omega)^{-1}_{\epsilon_1,\epsilon_2}=C_s(\omega)^{-1}_{\epsilon_1,\epsilon_2}-J(\mathbf{q}). \tag{16}$$

The leading in $1/D$ contributions to the effective spin cumulant contain diagrams of the form illustrated for the on-site self-energy in Fig. 2. This again follows from the power counting rules of Appendix A and can be derived following a procedure parallel to that of Appendix B. As a result, all the loops involving intersite interactions are equal to the corresponding Weiss fields $\chi^{-1}_{s,0}$ and $\chi^{-1}_{ch,0}$.

The above, in turn, implies that the quantity C_s we have just defined for the lattice model is also equal to the sum of all the diagrams for the local spin susceptibility of the effective impurity problem, Eq. (5), which are not reducible by cutting a single $\chi^{-1}_{s,0}$ line. The local spin susceptibility then satisfies the following equation,

$$\begin{aligned}\chi_{s,loc}(\epsilon_1,\epsilon_2;\omega)=&C_s(\epsilon_1,\epsilon_2;\omega)\\&+\int d\epsilon'\int d\epsilon'' C_s(\epsilon_1,\epsilon';\omega)\chi^{-1}_{s,0}(\omega)\\&\times\chi_s(\epsilon'',\epsilon_2;\omega)\end{aligned} \tag{17}$$

as illustrated in Fig. 5. Equation (17) leads to

$$C_s(\omega)^{-1}_{\epsilon_1,\epsilon_2}=\chi_{s,loc}(\omega)^{-1}_{\epsilon_1,\epsilon_2}+\chi^{-1}_{s,0}(\omega), \tag{18}$$

which specifies how to calculate the effective spin cumulant from the Weiss field and the local spin susceptibility.

Combining Eqs. (16), (14), and (18), we derive the following form for the momentum-dependent irreducible vertex function,

$$\begin{aligned}I(\epsilon_1,\epsilon_2;\mathbf{q},\omega)=&\chi^{ph}(\epsilon_1;\omega)^{-1}\delta_{\epsilon_1,\epsilon_2}-\chi_{s,loc}(\omega)^{-1}_{\epsilon_1,\epsilon_2}\\&-\chi^{-1}_{s,0}(\omega)+J(\mathbf{q})\end{aligned} \tag{19}$$

as well as the local irreducible vertex function $I_{loc}(\epsilon_1\epsilon_2;\omega)\equiv\Sigma_{\mathbf{q}}I(\epsilon_1,\epsilon_2;\mathbf{q},\omega)$,

$$\begin{aligned}I_{loc}(\epsilon_1,\epsilon_2;\omega)=&\chi^{ph}(\epsilon_1;\omega)^{-1}\delta_{\epsilon_1,\epsilon_2}-\chi_{s,loc}(\omega)^{-1}_{\epsilon_1,\epsilon_2}\\&-\chi^{-1}_{s,0}(\omega).\end{aligned} \tag{20}$$

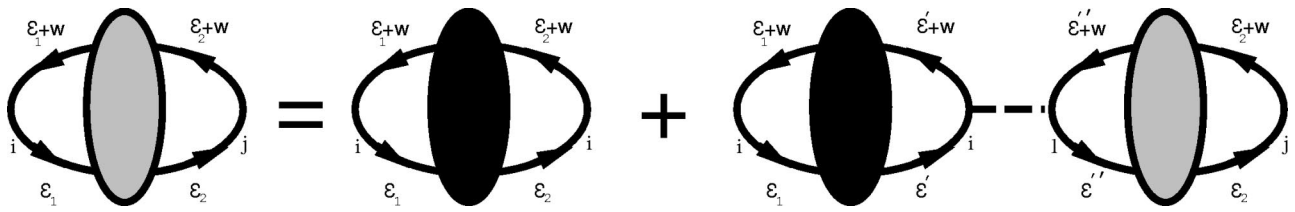

FIG. 4. Susceptibility expansion in terms of cumulants. The bubble with a shaded insertion represents the susceptibility, while the bubble with a solid insertion corresponds to an effective two-particle cumulant.

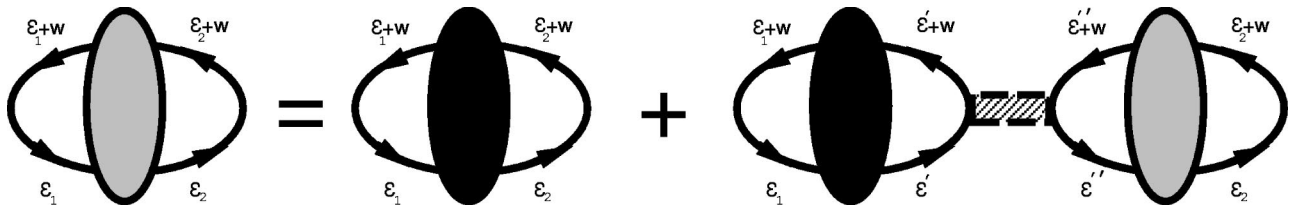

FIG. 5. Local susceptibility expansion in terms of cumulants and the Weiss field.

B. Correlation functions

We now proceed to determine the momentum-dependent correlation function. Again, we focus on the spin susceptibility.

Integrating both sides of Eq. (15) over both ϵ_1 and ϵ_2 leads to the following,

$$\chi_{s,ij}(\omega)=M_s(\omega)\delta_{ij}+\sum_l M_s(\omega)J_{il}\chi_{s,lj}(\omega), \qquad (21)$$

where the integrated spin cumulant $M_s(\omega) \equiv \int d\epsilon_1 \int d\epsilon_2 C_s(\epsilon_1,\epsilon_2;\omega)$. Equation (21) yields,

$$\chi_s(\mathbf{q},\omega)=\frac{M_s(\omega)}{1-J(\mathbf{q})M_s(\omega)}. \qquad (22)$$

The integrated spin cumulant $M_s(\omega)$ can be determined from integrating both sides of Eq. (17) over both ϵ_1 and ϵ_2,

$$\chi_{s,loc}(\omega)=M_s(\omega)+M_s(\omega)\chi_{s,0}^{-1}(\omega)\chi_{s,loc}(\omega), \qquad (23)$$

which yields,

$$M_s(\omega)=\frac{\chi_{s,loc}(\omega)}{1+\chi_{s,0}^{-1}(\omega)\chi_{s,loc}(\omega)}. \qquad (24)$$

Inserting Eq. (24) into Eq. (22) leads to the final form for the momentum-dependent correlation function,

$$\chi_s(\mathbf{q},\omega)=\frac{1}{1/\chi_{s,loc}(\omega)+\chi_{s,0}^{-1}(\omega)-J(\mathbf{q})}. \qquad (25)$$

Equation (25) is one of the most important conclusions of this paper. It specifies how to calculate the momentum-dependent spin susceptibility from the local spin susceptibility, the Weiss field [$\chi_{s,0}^{-1}$, see Eq. (4)], and the exchange interaction. As a check for the validity of this expression, one may rewrite it in the following form,

$$\chi_s(\mathbf{q},\omega)=\chi_{s,loc}(\omega)+\chi_{s,loc}(\omega)[J(\mathbf{q})-\chi_{s,0}^{-1}(\omega)]\chi_s(\mathbf{q},\omega). \qquad (26)$$

By using the expression for the Weiss field $\chi_{s,0}^{-1}$, Eq. (4), it is straightforward to see that summing both sides of Eq. (26) over $\mathbf{q}$ leads to $\chi_{s,loc}=\chi_{s,loc}$. An alternative derivation of Eq. (25) is given in Appendix C.

IV. CONSERVING CRITERIA

We see from the above that the single-particle self-energy is local, but the two-particle vertex function is momentum dependent. We show in this section that, in spite of this, the approach is conserving.

An approach is conserving if both the single-particle self energy and two-particle irreducible vertex functions are functional derivatives of the Luttinger-Ward Φ-potential with respect to the single-particle Green's functions.[12] The latter is defined as the sum of all closed skeleton diagrams, and is a functional of the single-particle Green's function and interaction parameters. Applying this criterion to our case is somewhat subtle. The momentum-dependent part of the vertex function comes from diagrams for the Luttinger-Ward potential that are subleading in $1/D$. These include the Hartree and Fock contributions. In fact, due to the usage of normal-ordered operators in the Hamiltonian the Hartree contributions to Luttinger-Ward potential and to the self-energy, given in Figs. 6(a) and 6(b) respectively, are identically zero. The corresponding Fock contributions, also given in Figs. 6(a) and 6(b), respectively, are subleading in $1/D$. At the same time, both the Hartree and Fock contributions to the two-particle vertex functions, given in Fig. 6(c), are of leading order: Their contributions to $I_{\langle ij\rangle}$ are of order $1/\sqrt{D}$.

Because of this subtlety, we use an alternate set of conserving criteria introduced in Ref. 13. Two conditions are sufficient for an approach to be conserving. The first states $G_2(1,3,1^+,3^+)=G_2(3,1,3^+,1^+)$, where G_2 is the standard two-particle Green's function. [In this section we follow the short-hand notation of Ref. 13. For instance, 1 labels $(\mathbf{x}_1,\tau_1)$, and 1^+ labels $(\mathbf{x}_1,\tau_1+0^+)$.] This condition is satisfied in our case.

The second condition relates the single-particle self-energy and the reducible two-particle vertex function. This condition contains two equations, one derived from the equation of motion, $\partial_{\tau_1}G(1,1')=[G(1,1'),H]$, and the other its

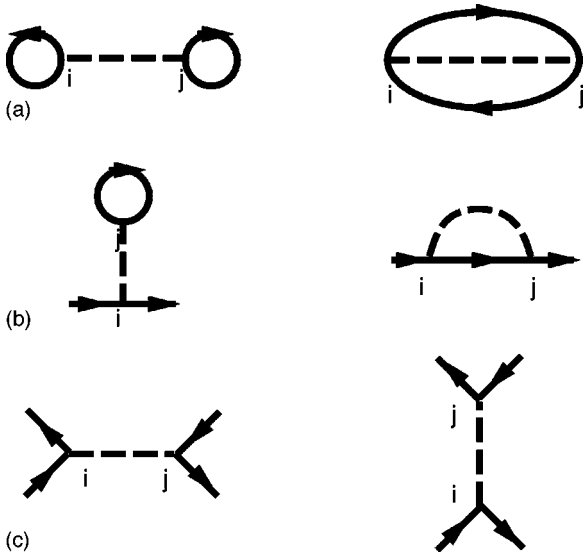

FIG. 6. Hartree and Fock contributions to (a) the Luttinger-Ward potential; (b) the self-energy; and (c) the vertex function.

adjoint. In what follows, we show that the first equation is satisfied; similar arguments establish the validity of the second equation. In addition, for notational simplicity, we consider the case when only the intersite density-density interaction v_{ij} is finite (the conclusion is unchanged if J_{ij} is also present). In this case, the condition for the Hamiltonian given by Eq. (1) has the following form,

$$\Sigma(1,1')=-\int d\bar{3}d\bar{5}d\bar{6}d\bar{8}v_{x_1,x_3}[G(1,\bar{3})\delta(\bar{3}-1') + G(1,\bar{5})G(\bar{3},\bar{6})\Gamma(\bar{5},\bar{6},1',\bar{8})G(\bar{8},\bar{3})] - \int d\bar{5}d\bar{6}d\bar{8}U[\delta(1-1')n_{-\sigma}(1) + G(1,\bar{5})G(1,\bar{6})\Gamma(\bar{5},\bar{6},1',\bar{8})G(\bar{8},1)], \quad (27)$$

where Γ is the reducible two-particle vertex function.[14]

Consider first the case when $\mathbf{x}_1$ is nearest neighbor to $\mathbf{x}_{1'}$. A contribution is of leading order if it is of order $1/\sqrt{D}$. The left-hand side is of order $1/D$ and hence subleading. The right-hand side contains the nonlocal component of the vertex function; one might then worry about whether it is still subleading. That it is so can be seen by enumerating the possible spatial locations of the integration variables and using the rules of Appendix A. In fact, the dominant contributions are all of order $1/D$ and, hence, the right-hand side is also subleading. We illustrate this with two examples. Consider first the case $\mathbf{x}_{\bar{3}}=\mathbf{x}_{\bar{6}}=\mathbf{x}_{\bar{8}}=\mathbf{x}_1$, and $\mathbf{x}_{\bar{5}}=\mathbf{x}_{1'}$, which contribute to the second term on the right-hand side of Eq. (27). The nonlocal vertex function $\Gamma(1',1,1',1)$, which is of order $1/\sqrt{D}$, is accompanied by another nonlocal Green's function, $G(1,1')$, which is also of order $1/\sqrt{D}$. Consider next the contribution from the first term on the right-hand side of Eq. (27), with $\mathbf{x}_{\bar{5}}=\mathbf{x}_{1'}$ and $\mathbf{x}_{\bar{3}}=\mathbf{x}_{\bar{6}}=\mathbf{x}_{\bar{8}}=\mathbf{x}_l$, where $\mathbf{x}_l$ is nearest-neighbor to $\mathbf{x}_1$. Again, the non-local vertex function $\Gamma(1',l,1',l)$, which is now of order $1/D$, is accompanied by $G(1,1')$ and v_{x_1,x_l}, both of which are of order $1/\sqrt{D}$; summing over l gives rise to a factor D, leading to an overall $1/D$ contribution. We conclude that to leading order, Eq. (27) is indeed satisfied. Analogous arguments apply to arbitrary $\mathbf{x}_1 \neq \mathbf{x}_{1'}$.

Consider next $\mathbf{x}_1=\mathbf{x}_{1'}$. The leading-order here corresponds to O(1). To this leading order Eq. (27) becomes,

$$\Sigma(1,1)=-\int d\bar{3}v_{x_1,x_{\bar{3}}}G(1,1)G(\bar{3},\bar{3})\Gamma(1,\bar{3},1,\bar{3})G(\bar{3},\bar{3}) - U[n_{-\sigma}(1)+G(1,1)G(1,1)\Gamma(1,1,1,1)G(1,1)]. \quad (28)$$

[For notational simplicity, we have suppressed the time indices.] Here, the right-hand side also contains the nonlocal components of the vertex function Γ. We can expand the right-hand side in terms of the bare intersite interaction by expressing Γ in terms of the irreducible vertex function I and using Eqs. (19) and (20). This leads to diagrams that are in one to one correspondence with those for the on-site self energy. Equation (28) is then satisfied as well.

To summarize, in order to correctly derive the leading-order irreducible vertex function by differentiating the Luttinger-Ward potential, it is necessary to keep not only the leading in $1/D$ contributions to the Luttinger-Ward potential but also the Hartree-Fock-type terms, which are formally subleading. The $D\rightarrow\infty$ limit has to be taken after differentiating the Luttinger-Ward potential with respect to the Green's functions. The process of taking a functional derivative of a diagram with respect to the single-particle Green's function can change the order in $1/D$. In spite of these complications, we established that the approach still satisfies the criteria of Ref. 13 and, hence, is conserving.

V. DISCUSSIONS

A. Multiband models and ordered states

The generalization of our approach to multiband cases is straightforward. For a two-band extended Hubbard model, the corresponding mean field equations have already been written down in Refs. 7 and 8.

Another important two-band model is the Kondo lattice model,

$$H=\sum_{\langle ij\rangle,\sigma} t_{ij}c_{i\sigma}^{\dagger}c_{j\sigma}+\sum_i J_K\vec{S}_i\cdot\vec{s}_{c_i}-\sum_{\langle ij\rangle} J_{ij}\vec{S}_i\cdot\vec{S}_j, \quad (29)$$

where $\vec{S}_i$ denotes an impurity spin at site i, and $\vec{s}_{c_i}$ represents the spin of conduction $(c-)$ electrons at site i. Taking the large D limit, again with $t_{ij}=t_0/\sqrt{D}$ and $J_{ij}=J_0/\sqrt{D}$, results in the following effective impurity action,

$$S^{MF}=S_{top}+\int_0^\beta d\tau J_K\vec{S}\cdot\vec{s}_c-\int_0^\beta d\tau\int_0^\beta d\tau' \times\Big[\sum_\sigma c_\sigma^{\dagger}(\tau)G_0^{-1}(\tau-\tau')c_\sigma(\tau') + \vec{S}(\tau)\cdot\chi_{s,0}^{-1}(\tau-\tau')\vec{S}(\tau')\Big], \quad (30)$$

where S_{top} describes the Berry-phase of the impurity spin. The Weiss fields G_0^{-1} and $\chi_{s,0}^{-1}$ are determined by the self-consistency equations as given in Eqs. (8) and (4). The effective action can equivalently be written in terms of the following impurity problem,

$$H_{imp}=\sum_{k\sigma} E_k\eta_{k\sigma}^{\dagger}\eta_{k\sigma}+\sum_q w_q\vec{\phi}_q^{\dagger}\cdot\vec{\phi}_q-\mu\sum_\sigma c_\sigma^{\dagger}c_\sigma + t\sum_{k\sigma}(c_\sigma^{\dagger}\eta_{k\sigma}+\text{H.c.})+J_K\vec{S}\cdot\vec{s}_c + g\sum_q\vec{S}\cdot(\vec{\phi}_q+\vec{\phi}_{-q}^{\dagger}), \quad (31)$$

where E_k, t, w_q and g may be determined from the Weiss fields G_0^{-1} and $\chi_{s,0}^{-1}$ as specified by Eq. (10).

Finally, we can also extend the approach to a state with long-range commensurate spatial ordering. This requires taking the normal ordering, as specified in Eq. (1), with a site-dependent average charge or spin appropriate for the ordered state. The dynamical mean field equations, Eqs. (5), (8), and (4) still apply.

B. Incommensurate susceptibilities

The form of the momentum-dependent correlation function given by Eq. (25) applies to generic $\mathbf{q}$. The momentum dependence is entirely given by that of the corresponding intersite interaction. It does not depend on the single-particle dispersion.

The situation is different from the standard large D limit, where the momentum dependence of the correlation functions is given entirely by the single-particle dispersion. The latter is possible for lattices with unbounded bare density of states — such as hypercubic lattice—which contains special $\mathbf{q}$ such that $\epsilon_q = \Sigma_{ij} e^{i\mathbf{q}\cdot\mathbf{R}_{ij}} t_{ij}$ is of order $\sqrt{D}$.

Formally, the extended DMFT described here can only be defined for lattices with a bounded bare density of states. It becomes ill defined for lattices with unbounded density of states: When ϵ_q is of order $\sqrt{D}$, so is $J(\mathbf{q})$; through the form of the susceptibility, Eq. (25), the system would then become unstable [when $J(\mathbf{q})$ is positive].

One way to approximately incorporate the incommensurate fluctuations induced by Fermi-surface features is through the (exact) Bethe-Salpeter equation

$$\chi_s(\mathbf{q},\omega)^{-1}_{\epsilon_1,\epsilon_2} = \chi^{ph}(\epsilon_1;\mathbf{q},\omega)^{-1}\delta_{\epsilon_1,\epsilon_2} - I(\epsilon_1,\epsilon_2;\mathbf{q},\omega), \tag{32}$$

where $\chi^{ph}(\epsilon_1;\mathbf{q},\omega)$ is the usual particle-hole susceptibility bubble calculated in terms of the full single-particle propagators. One still uses the extended DMFT to calculate the self-energy and the irreducible vertex function, Eq. (19). At the same time, one adopts the momentum-dependence of χ^{ph} and the intersite interactions in a given system at finite dimensions. This procedure is of course no longer exact.

C. Comparison with other approaches

A direct $1/D$ expansion has been introduced by Schiller and Ingersent.[15] The expansion is carried out for the Luttinger-Ward Φ-potential,[16] i.e., all the closed skeleton diagrams. The leading $(1/D^0)$ order contributions involve, as usual, only a single site. The next-to-leading order $(1/D)$ contributions come from diagrams involving two sites. A dynamical mean field description to this level requires two effective actions describing a single impurity and a two-impurity cluster, each coupled to its respective self-consistent medium. Similarly, expanding to order $1/D^n$ requires solving simultaneously effective problems involving one-site, two-site, and up to $n+1$ site clusters, each embedded in its own self-consistent medium.

The extended DMFT described here can be thought of as a conserving resummation of contributions to all orders in $1/D$. This is illustrated in Fig. 7. A detailed comparison between the two approaches should in principle be meaningful when spatial correlations are short ranged.

An alternative approach has recently been introduced by Hettler *et al.*[17] In this approach, the Brillouin zone is divided into N_c regions. For each frequency, one introduces one Weiss field for each momentum region. The resulting self-consistent problem describes an N_c-site cluster embedded in these N_c self-consistent Weiss fields. For $N_c = 1$, it reduces to the standard large D DMFT. The precise relationship between their approach and the extended DMFT described here is unclear.

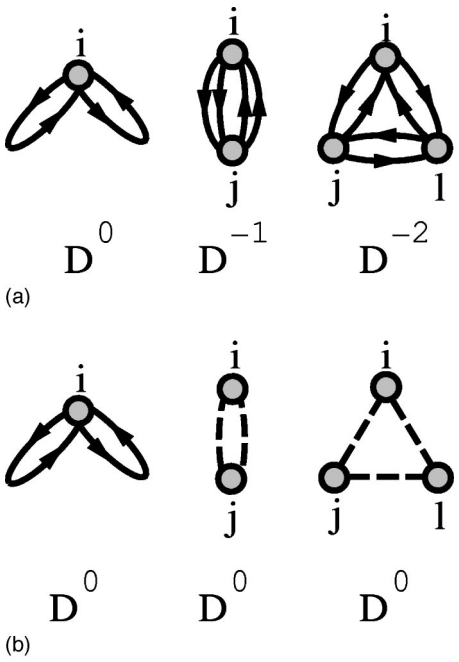

FIG. 7. (a) Single-site, two-site, and three-site diagrams for the Luttinger-Ward potential in a direct expansion in $1/D$; (b) The corresponding diagrams in the extended DMFT.

Finally, our approach also has some similarities with the dynamical mean field theory of random spin systems. Bray and Moore[18] considered the quantum Sherrington-Kirkpatrick model, in which the exchange coupling is infinite ranged and has a Gaussian distribution of mean zero and variance scaled to J^2/N where N is the size of the system. Carrying out disorder averaging using replicas, as usual, leads to a problem with four-spin interactions; each spin now carries a replica index. Since the exchange couplings associated with different bonds are uncorrelated, the four spin interaction has the form of two spins at different times τ and τ', from any site, interact with two other spins, also at τ and τ', at every other site. Introducing a Hubbard-Stratonovich decomposition and taking the $N\to\infty$ limit then leads to a single-site problem with retarded spin-spin interactions. In the paramagnetic phase, the effective impurity problem has a similar form as the spin part of Eq. (5), with a self-consistency equation which is also similar—though not identical—to Eq. (4). Generalizing[19,20] to the case when conduction electrons are also present gives rise to mean field equations similar to those described here. The form of correlation functions is of course very different.

VI. CONCLUSIONS

To summarize, we have presented a perturbative derivation of the extended dynamical mean-field theory. This approach goes beyond the standard $D=\infty$ DMFT by incorporating the quantum fluctuations associated with intersite interactions.

The self-consistent impurity problem has the form of an Anderson impurity model with additional bosonic baths.

This is a novel kind of impurity problem, and is of interest in its own right. The role of a scalar boson bath is to introduce additional screening, thereby enhancing orthogonality. The precise consequences of the enhanced screening depends on the form of the spectral function of the bosons. Reference 7 analyzed an impurity problem containing both a scalar boson bath with a spectral function of ω^γ and a conduction electron band with a regular density of states at its Fermi energy. The correlation functions have mean-field exponents. The effect of an anisotropic vector-boson bath is similar to the scalar case. The effect of an isotropic vector-boson bath is more complex. We and, independently, Sengupta have carried out[8,21] a renormalization group analysis of spins coupled both to a regular conduction electron band (J_K) and to a vector-boson bath (g) with a spectral function of ω^γ. In the subohmic case ($\gamma<1$), there exists a critical point separating a phase characterized by the fixed point at $J_K^*=\infty, g^*=0$ and another by $J_K^*=0, g^*\sim\sqrt{1-\gamma}$. The critical exponents are anomalous.[21] In the absence of conduction electrons, the impurity problem corresponds to a spin coupled to vector bosons alone. Sachdev and Ye (Ref. 22) solved such a model in the large N limit (see also Ref. 23). Finally, we note that quantum Monte Carlo methods have recently been developed for this type of impurity problems.[24]

The momentum-dependent correlation functions in the extended DMFT have the general form given by Eq. (25). While different in details, it is similar to the phenomenological expression recently introduced in Refs. 25 and 26 in the context of the dynamical spin susceptibility in a heavy fermion metal ($CeCu_{6-x}Au_x$) close to a zero-temperature phase transition. The experiments[25,27] at the critical concentration are suggestive of a dynamical spin susceptibility $[J(\mathbf{q})+f(\omega,T)]^{-1}$ over the entire Brillouin zone, where the frequency and temperature dependence in $f(\omega,T)$ show an anomalous exponent. Whether a quantum critical point with an anomalous exponent in the dynamical susceptibility can emerge in the extended DMFT described here is an exciting open question.[29]

Finally, the extended DMFT described here should be applicable to quantitatively study the short, but finite, ranged dynamical fluctuations in paramagnetic phases (whether or not the ground state is ordered). Consider, for example, the spin fluctuations in the paramagnetic phase of a Mott insulator. In the standard large D limit, these fluctuations simply reflect isolated local moments: They contain no damping and are featureless in momentum space. In the extended DMFT, the self-consistent problem contains mode coupling and hence damping. In addition, through Eq. (25) the dynamical spin susceptibility is expected to be peaked at antiferromagnetic wave vectors. The extended DMFT is particularly useful at temperatures where the correlation length is short; here other approaches which take into account only long-wavelength fluctuations would break down. Quantitative calculations using the extended DMFT will perhaps allow a detailed understanding of the neutron scattering results in both undoped and doped Mott insulators, such as V_2O_3 (Ref. 28) where the exchange interactions are not particularly large.

ACKNOWLEDGMENTS

We would like to thank G. Kotliar and D. Vollhardt for useful discussions. This work has been supported in part by NSF Grant No. DMR-9712626, Research Corporation, and A. P. Sloan Foundation.

FIG. 8. A diagram for the on-site self-energy. It connects the selected site to the rest of the lattice by three interaction lines, making it subleading.

APPENDIX A: POWER COUNTING RULES

The order in $1/D$ of the correlation functions and vertex functions can be determined by analyzing the diagrams in real space.

Consider first the single particle Green's function G_{ij} and vertex functions I_{ijij} and Γ_{ijij}. In any real space Feynman diagrams for these quantities, it takes at least $||i-j||$ number of fermion propagation or intersite interaction steps. Therefore, $G_{ij}\sim I_{ijij}\sim\Gamma_{ijij}\sim O(1/D)^{||i-j||/2}$.

Consider next the vertex functions involving three independent sites, $I(i,j,i,l)$ and $\Gamma(i,j,i,l)$. Every diagram involves at least three independent paths of fermion propagators and/or interaction lines. Its order in $1/D$ is smaller than what corresponds to two bonds connecting one site to the two remaining sites. Therefore, $I(i,j,i,l)\sim\Gamma(i,j,i,l)\sim o(1/D)^{M_3/2}$ where $M_3=\min(||i-j||+||i-l||,||i-j||+||j-l||,||i-l||+||j-l||)$.

Finally, consider the vertex functions involving four independent sites, $I(i,j,l,m)$ and $\Gamma(i,j,l,m)$. Every diagram involves at least four independent paths of fermion propagators and/or interaction lines. As a result, $I(i,j,l,m)\sim\Gamma(i,j,l,m)\sim o(1/D)^{M_4/2}$ where M_4 is the minimum of the sum of the lengths of three bonds connecting all four sites. (The three bonds can either terminate at one site or form a continuous path between two different sites.)

APPENDIX B: ON-SITE SELF-ENERGY

Consider an arbitrary skeleton expansion diagram for the on-site self energy for site 0, $\Sigma_{00}(\omega)$. From the counting rules of Appendix A, only local fermion propagators appear. The only non-local terms involve intersite interactions. These intersite interaction terms can be grouped into separate loops, each starting at site 0 and returning to site 0 as is illustrated in Fig. 2(a). Note that, no loop can return to site 0 more than once. For instance, a contribution given in Fig. 8 is subleading.

The analytic expression for each loop can be determined as follows. The beginning and ending interaction lines give a product $J_{0l}J_{m0}$, where l and m are arbitrary sites nearest-neighbor to site 0. The solid square then represents a correlation function involving $\vec{S}_l$ and $\vec{S}_m$. Given that site 0 is excluded from anywhere in the solid square, this correlation function has to be evaluated in terms of $H^{(0)}$, defined as the original Hamiltonian Eq. (1) with site 0 excluded. As a result, this loop can be written as

$$\sum_{lm} J_{0l}J_{m0}\chi^{(0)}_{lm}, \tag{B1}$$

where $\chi^{(0)}_{lm}=\langle T_\tau \vec{S}_l(\tau)\cdot\vec{S}_m(\tau')\rangle_{H^{(0)}}$, which can be determined as follows. For $\chi_{lm}=\langle T_\tau \vec{S}_l(\tau)\cdot\vec{S}_m(\tau')\rangle_H$, the cumulant expansion given in Eq. (15) implies that its Fourier transform satisfies $\chi_{lm}=\chi_{ll}\chi'_{lm}\chi_{mm}$, where $\chi'_{lm}\equiv\Sigma_{paths}J_{ll_1}\chi_{l_1l_1}J_{l_1l_2}\chi_{l_2l_2}\cdots\chi_{l_nl_n}J_{l_nm}$ and $[l,l_1,l_2,\ldots,l_n,m]$ labels a non-self-retracing path from site l to site m. This in turn implies $\chi^{(0)}_{lm}=\chi_{lm}-\chi_{ll}\chi'_{l0}\chi_{00}\chi'_{0m}\chi_{mm}$. Therefore,

$$\chi^{(0)}_{lm}=\chi_{lm}-\chi_{l0}\chi_{0m}/\chi_{00} \tag{B2}$$

leading to the expression for the spin Weiss field, $\chi^{-1}_{s,0}$, given in Eq. (4).

Similarly, an interaction chain generated by v_{ij} corresponds to the charge Weiss field, $\chi^{-1}_{ch,0}$, given in Eq. (4).

APPENDIX C: ALTERNATIVE DERIVATION OF THE MOMENTUM-DEPENDENT SUSCEPTIBILITY

In this section we present an alternative derivation for the momentum-dependent susceptibility $\chi(\mathbf{q},\omega)$, Eq. (25).

We re-write Eq. (4) in momentum space,

$$\chi_0^{-1}(\omega)=\sum_q J^2(\mathbf{q})\chi(\mathbf{q},\omega) - \left[\sum_q J(\mathbf{q})\chi(\mathbf{q},\omega)\right]^2 \Big/ \chi_{loc}(\omega). \tag{C1}$$

In addition, we use Eq. (22), i.e.,

$$\chi(\mathbf{q},\omega)=\frac{1}{M(\omega)^{-1}-J(\mathbf{q})}. \tag{C2}$$

We now substitute Eq. (C2) into Eq. (C1). By using

$$\sum_q \frac{J(\mathbf{q})}{M(\omega)^{-1}-J(\mathbf{q})}=-1+M(\omega)^{-1}\chi_{loc}(\omega) \tag{C3}$$

and

$$\sum_q \frac{J(\mathbf{q})^2}{M(\omega)^{-1}-J(\mathbf{q})}=M(\omega)^{-1}[-1+\chi_{loc}(\omega)] \tag{C4}$$

we obtain $\chi_0^{-1}(\omega)=M(\omega)^{-1}-1/\chi_{loc}(\omega)$, i.e.,

$$M(\omega)^{-1}=1/\chi_{loc}(\omega)+\chi_0^{-1}(\omega). \tag{C5}$$

Inserting Eq. (C5) into Eq. (C2) then leads to Eq. (25).

Note that, Eq. (25) reduces to the correct result for generic $\mathbf{q}$ in the standard large D limit where $J(\mathbf{q})=0$ and $\chi_0^{-1}=0$.

[1] S. Doniach, Physica B **91**, 231 (1977).

[2] B. A. Jones, C. M. Varma, and J. W. Wilkins, Phys. Rev. Lett. **61**, 125 (1988).

[3] *Proceedings of the ITP Conference on Non-Fermi Liquid Behavior in Metals, Santa Barbara, 1996*, edited by P. Coleman, B. Maple, and A. J. Millis [J. Phys.: Condens. Matter, **8** (1996)].

[4] *The Metallic and Nonmetallic States of Matter*, edited by P. P. Edwards and C. N. R. Rao (Taylor & Francis, London, 1985); *Metal-Insulator Transitions Revisited* (Taylor & Francis, London, 1995).

[5] For an earlier review, see A. Georges, G. Kotliar, W. Krauth, and M. J. Rozenberg, Rev. Mod. Phys. **68**, 13 (1996).

[6] W. Metzner and D. Vollhardt, Phys. Rev. Lett. **62**, 324 (1989).

[7] Q. Si and J. L. Smith, Phys. Rev. Lett. **77**, 3391 (1996).

[8] J. L. Smith and Q. Si, Europhys. Lett. **45**, 228 (1999); cond-mat/9705140 (unpublished).

[9] H. Kajueter and G. Kotliar (private communication); H. Kajueter, Ph.D. thesis, Rutgers University, 1996.

[10] The Hartree contributions influence the energetics of spatially ordered states. See, for example, P. J. van Dongen, Phys. Rev. Lett. **74**, 182 (1995); D. Vollhardt *et al.*, Z. Phys. B: Condens. Matter **103**, 283 (1997).

[11] W. Metzner, Phys. Rev. B **43**, 8549 (1991).

[12] G. Baym, Phys. Rev. **127**, 1391 (1962).

[13] G. Baym and L. P. Kadanoff, Phys. Rev. **124**, 287 (1961).

[14] We note that the Fock self-energy diagram (for $\mathbf{x}_1$ nearest neighbor to $(\mathbf{x}_{1'})$ $v_{x_1,x_{1'}}G(1,1')$ appears on the right-hand side and is subleading ($\propto 1/D$).

[15] A. Schiller and K. Ingersent, Phys. Rev. Lett. **75**, 113 (1995).

[16] The expansion for Φ was first introduced in E. Halvorsen, G. S. Uhrig, and G. Czycholl, Z. Phys. B: Condens. Matter **94**, 291 (1994). These authors considered a spinless one-band model. The absence of any on-site interaction in this model makes it possible to explicitly enumerate all contributions to order $1/D$; a cluster expansion is not necessary in this special case.

[17] M. H. Hettler, A. N. Tahvildar-Zadeh, M. Jarrell, T. Pruschke, and H. R. Krishnamurthy, Phys. Rev. B **58**, 7475 (1998).

[18] A. J. Bray and M. A. Moore, J. Phys. C **13**, L655 (1980).

[19] S. Sachdev, N. Read, and R. Oppermann, Phys. Rev. B **52**, 10 286 (1995).

[20] A. M. Sengupta and A. Georges, Phys. Rev. B **52**, 10 295 (1995).

[21] A. M. Sengupta, cond-mat/9707316.

[22] S. Sachdev and J. Ye, Phys. Rev. Lett. **70**, 3339 (1993).

[23] O. Parcollet and A. Georges, Phys. Rev. B **59**, 5341 (1999).

[24] D. R. Grempel and M. J. Rozenberg, Phys. Rev. B **60**, 4702 (1999).

[25] A. Schroder, G. Aeppli, E. Bucher, R. Ramazashvili, and P. Coleman, Phys. Rev. Lett. **80**, 5623 (1998).
[26] P. Coleman, Physica B **258–261**, 353 (1999).
[27] O. Stockert, H. von Löhneysen, A. Rosch, N. Pyka, and M. Loewenhaupt, Phys. Rev. Lett. **80**, 5627 (1998).
[28] W. Bao, C. Broholm, G. Aeppli, S. A. Carter, P. Dai, T. F. Rosenbaum, J. M. Honig, P. Metcalf, and S. F. Trevino, Phys. Rev. B **58**, 12 727 (1998).
[29] More recent discussions can be found in Q. Si, J. L. Smith, and K. Ingersent, Int. J. Mod. Phys. B **13**, 2331 (1999).